



ARL-TR-9346 • Nov 2021



Adaptive Control for a Guided Projectile with High-Order Actuator Dynamics Using an Expanded Reference Model

by Benjamin C Gruenwald and Joshua T Bryson

Approved for public release; distribution is unlimited.

NOTICES

Disclaimers

The findings in this report are not to be construed as an official Department of the Army position unless so designated by other authorized documents.

Citation of manufacturer's or trade names does not constitute an official endorsement or approval of the use thereof.

Destroy this report when it is no longer needed. Do not return it to the originator.



Adaptive Control for a Guided Projectile with High-Order Actuator Dynamics Using an Expanded Reference Model

by Benjamin C Gruenwald and Joshua T Bryson
*Weapons and Materials Research Directorate,
DEVCOM Army Research Laboratory*

REPORT DOCUMENTATION PAGE

Form Approved
OMB No. 0704-0188

Public reporting burden for this collection of information is estimated to average 1 hour per response, including the time for reviewing instructions, searching existing data sources, gathering and maintaining the data needed, and completing and reviewing the collection information. Send comments regarding this burden estimate or any other aspect of this collection of information, including suggestions for reducing the burden, to Department of Defense, Washington Headquarters Services, Directorate for Information Operations and Reports (0704-0188), 1215 Jefferson Davis Highway, Suite 1204, Arlington, VA 22202-4302. Respondents should be aware that notwithstanding any other provision of law, no person shall be subject to any penalty for failing to comply with a collection of information if it does not display a currently valid OMB control number.

PLEASE DO NOT RETURN YOUR FORM TO THE ABOVE ADDRESS.

1. REPORT DATE (DD-MM-YYYY) November 2021		2. REPORT TYPE Technical Report		3. DATES COVERED (From - To) 1 May–31 August 2021	
4. TITLE AND SUBTITLE Adaptive Control for a Guided Projectile with High-Order Actuator Dynamics Using an Expanded Reference Model				5a. CONTRACT NUMBER	
				5b. GRANT NUMBER	
				5c. PROGRAM ELEMENT NUMBER	
6. AUTHOR(S) Benjamin C Gruenwald and Joshua T Bryson				5d. PROJECT NUMBER	
				5e. TASK NUMBER	
				5f. WORK UNIT NUMBER	
7. PERFORMING ORGANIZATION NAME(S) AND ADDRESS(ES) DEVCOM Army Research Laboratory ATTN: FCDD-RLW-WD Aberdeen Proving Ground, MD 21005				8. PERFORMING ORGANIZATION REPORT NUMBER ARL-TR-9346	
9. SPONSORING/MONITORING AGENCY NAME(S) AND ADDRESS(ES)				10. SPONSOR/MONITOR'S ACRONYM(S)	
				11. SPONSOR/MONITOR'S REPORT NUMBER(S)	
12. DISTRIBUTION/AVAILABILITY STATEMENT Approved for public release; distribution is unlimited.					
13. SUPPLEMENTARY NOTES primary author's email: <benjamin.c.gruenwald.civ@army.mil>. ORCID: Joshua Bryson, 0000-0002-0753-6823					
14. ABSTRACT In this report, a recently developed adaptive control architecture using an expanded reference model is generalized to account for high-order actuator dynamics. The features of this approach allow the verification of feasible actuator dynamics using linear matrix inequalities such that the adaptive control can correctly suppress the system uncertainties in the presence of actuator dynamics. Simulation studies are carried out on the longitudinal dynamics of a high-speed guided projectile model to demonstrate the capability of the expanded reference model adaptive control architecture to provide desirable performance in the presence of actuator dynamics.					
15. SUBJECT TERMS adaptive control, uncertain systems, actuator dynamics, projectile, high-speed flight					
16. SECURITY CLASSIFICATION OF:			17. LIMITATION OF ABSTRACT UU	18. NUMBER OF PAGES 24	19a. NAME OF RESPONSIBLE PERSON Benjamin C Gruenwald
a. REPORT Unclassified	b. ABSTRACT Unclassified	c. THIS PAGE Unclassified			19b. TELEPHONE NUMBER (Include area code) 410-306-0783

Contents

List of Figures	iv
List of Tables	iv
1. Introduction	1
2. Projectile Model	1
3. Model Reference Adaptive Control Architecture	4
4. Expanded Reference Model for High-Order Actuator Dynamics	5
5. Simulation Results	8
6. Conclusion	10
7. References	13
Appendix. Projection Operator	15
List of Symbols, Abbreviations, and Acronyms	17
Distribution List	18

List of Figures

Fig. 1	Illustration of the LTV flight body. Dimensions given in millimeters.	2
Fig. 2	Fin control surface configuration and deflection sign convention. View is from projectile base.....	3
Fig. 3	Nominal baseline control performance with no system uncertainty	9
Fig. 4	Nominal baseline control performance with system uncertainty included. Projectile response is unstable as expected.....	9
Fig. 5	Expanded reference model control performance for 1000% increase in the uncertainty of the pitch damping coefficient C_{m_q}	11
Fig. 6	Expanded reference model control performance for 1500% increase in the uncertainty of the pitch damping coefficient C_{m_q}	11
Fig. 7	Expanded reference model control performance for 2000% increase in the uncertainty of the pitch damping coefficient C_{m_q}	12
Fig. 8	Expanded reference model control performance for 2500% increase in the uncertainty of the pitch damping coefficient C_{m_q}	12

List of Tables

Table 1	Mass properties for LTV	2
Table 2	Aerodynamic parameters for LTV	3

1. Introduction

Recently, there has been increased interest on investigating technologies and methodologies to extend the range of guided munitions for improved battlefield coverage. Some of these include optimization of the munition aerodynamic design, analysis of control surface designs and actuator requirements, and trajectory shaping.¹⁻⁵ For the flight control designs of these guided munitions, adaptive control algorithms have been considered owing to their ability to suppress the effect of system uncertainties through the use of parameter estimates to tune control gains online.

An often neglected aspect in the design of these adaptive control architectures is the role the actuator dynamics play in limiting the achievable stability. This simplification is made by assuming the actuator dynamics are sufficiently fast such that the actuator output is, in a practical sense, equivalent to the desired input from the adaptive control law. However, since the adaptive control law relies on access to the system uncertainties and the actuator dynamics interfere with this direct access, if the actuator dynamics are not sufficiently fast, the capability of the adaptive control law to suppress the system uncertainties can be limited and instability can occur.

Recently Gruenwald et al.^{6,7} propose an approach using an expanded reference model such that the trajectories of this reference model are not significantly altered. Furthermore, recent work in Gruenwald and Bryson⁴ applied the expanded reference model approach to a fin-controlled guided munition. The limitation of the approach used in Gruenwald et al.^{4,6,7} is that only a first-order actuator model is considered. For more practical applications, it is more appropriate to consider the use of actuator dynamics represented in a high-order model. This report presents a generalization of the expanded reference model adaptive control architecture to account for high-order actuator dynamics. The proposed adaptive control architecture is applied to a high-speed guided projectile example using the longitudinal dynamics and a second-order actuator model.

2. Projectile Model

The Laboratory Technology Vehicle (LTV) is an engineering test-bed projectile used by the US Army Combat Capabilities Development Command (DEVCOM) Army Research Laboratory (ARL) to experiment with various gun-launched, guided flight and maneuver technologies. The LTV flight body was shaped through a series

of optimization analyses that identified design candidates with low drag and high length-to-diameter (L/D) ratios while maintaining marginal stability across the supersonic Mach regime.^{1,8,9} The body is 105 mm in diameter and 10 cal. (1.05 m) in length with a 0.5-cal. 7° boattail, and has a center of gravity (CG) located 5.6 cal. back from the nose. The projectile has a 30% ogive nose as a trade-off between drag and payload volume. There are four low-aspect-ratio fins arrayed symmetrically around the body. The projectile is designed to be sabot launched from an 8-inch-diameter gun with no deploying aerodynamic surfaces, which limits the fin span to 8 inches tip to tip. Figure 1 shows an illustration of the LTV flight body in a configuration with a 10.5-mm-radius rounded nose tip and 80-mm-chord control surfaces hinged at their leading edges. The mass properties for this variant are given in Table 1.

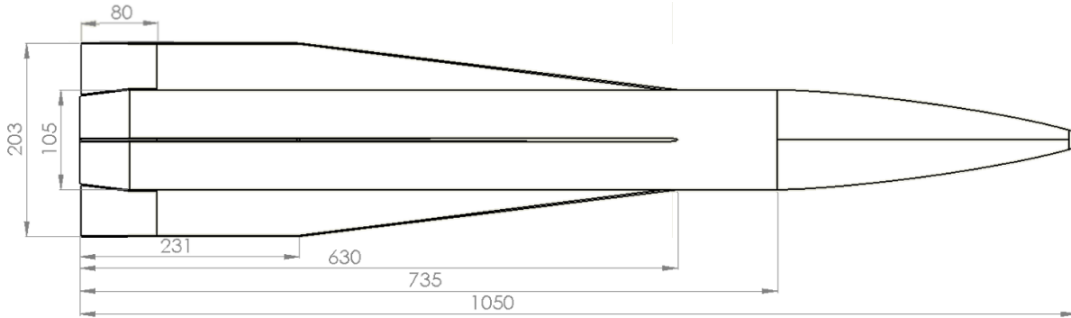


Fig. 1 Illustration of the LTV flight body. Dimensions given in millimeters.

Table 1 Mass properties for LTV

Mass Properties	Unit
Mass	16.8 kg
CGx	588 mm from nose
CGy, CGz	on center line
Ixx	0.0273 kg – m ³
Iyy, Izz	1.247 kg – m ³

For this analysis, the projectile is configured to fly in the “X” configuration with the roll angle location of movable surface i given by $\phi_{MAS}^i = [45^\circ, 135^\circ, 225^\circ, 315^\circ]$ for $\delta_1, \delta_2, \delta_3,$ and $\delta_4,$ respectively, as illustrated in Fig. 2.

In this work, the longitudinal dynamics of the projectile are considered. The linearized longitudinal aerodynamic model and pitch-plane equations of motion for

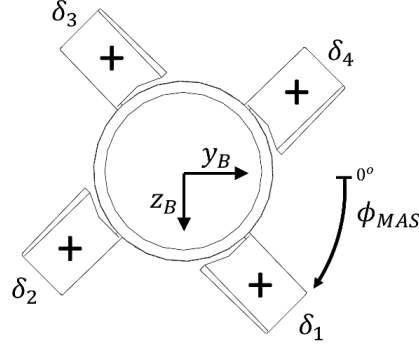


Fig. 2 Fin control surface configuration and deflection sign convention. View is from projectile base.

the projectile can be written as

$$\dot{q}(t) = \frac{QSD}{I_{zz}} \frac{D}{2V} C_{m_q} q(t) - \frac{mD}{I_{zz}} \frac{C_{m_\alpha}}{C_{Z_\alpha}} \dot{w}(t) + \frac{QSD}{I_{zz}} C_{m_{\delta_q}} \delta_q(t), \quad (1)$$

$$\ddot{w}(t) = -\frac{QS}{m} C_{Z_\alpha} q(t) + \frac{QS}{mV} C_{Z_\alpha} \dot{w}(t), \quad (2)$$

with the aerodynamic parameters given in Table 2. In addition, $q(t)$ denotes the pitch rate, $\dot{w}(t)$ denotes the translational acceleration in the pitch plane, and $\delta_q(t)$ denotes the deflection command in the pitch channel.

Table 2 Aerodynamic parameters for LTV

V	Total velocity of projectile
Q	Dynamic pressure, $\frac{1}{2}\rho V^2$
S, D	Aerodynamic reference area and aerodynamic reference diameter
m, ρ	Mass and air density
I_{zz}	Moment of inertia about body-frame z-axis
$C_{Z_\alpha}, C_{m_\alpha}, C_{m_q}$	Coefficients for Z-axis aerodynamic force, aerodynamic pitch moment, and pitch damping
$C_{m_{\delta_q}}$	Coefficient of control derivatives pitch

It then follows that Eqs. 1 and 2 can be written in compact form as

$$\dot{x}_0(t) = A_0 x_0(t) + B_0 u_0(t), \quad (3)$$

where $x_0(t) = [q(t), \dot{w}(t)]^T$ is the state vector, $u_0(t) = \delta_q(t)$ is the control signal,

and

$$A_0 = \begin{bmatrix} \frac{QSD}{I_{zz}} \frac{D}{2V} C_{m\dot{q}} & -\frac{mD}{I_{zz}} \frac{C_{m\alpha}}{C_{Z\alpha}} \\ -\frac{QS}{m} C_{Z\alpha} & \frac{QS}{mV} C_{Z\alpha} \end{bmatrix}, \quad B_0 = \begin{bmatrix} \frac{QSD}{I_{zz}} C_{m\delta_q} \\ 0 \end{bmatrix}.$$

3. Model Reference Adaptive Control Architecture

We now provide a brief overview of the standard model reference adaptive control problem in its generalized mathematical framework. For this purpose, consider the class of uncertain dynamical systems given by

$$\dot{x}(t) = Ax(t) + B(u(t) + W^T x(t)), \quad x(0) = x_0, \quad (4)$$

where $x(t) \in \mathbb{R}^n$ is the measurable state vector, $u(t) \in \mathbb{R}^m$ is the control signal, $A \in \mathbb{R}^{n \times n}$ and $B \in \mathbb{R}^{n \times m}$ are known system matrices and the pair (A, B) is controllable, and $W \in \mathbb{R}^{n \times m}$ is an unknown weight matrix. The linearized longitudinal dynamics for the LTV given by Eq. 3 fits the form of Eq. 4 where “ W ” captures any uncertainty in the aerodynamic coefficients.

Next, consider the reference model capturing a desired closed-loop dynamical system performance given by

$$\dot{x}_r(t) = A_r x_r(t) + B_r c(t), \quad x_r(0) = x_{r0}, \quad (5)$$

where $x_r(t) \in \mathbb{R}^n$ is the reference state vector, $A_r \in \mathbb{R}^{n \times n}$ is the Hurwitz reference model matrix, $B_r \in \mathbb{R}^{n \times m}$ is the command input matrix, and $c(t) \in \mathbb{R}^m$ is the desired uniformly continuous smooth and bounded reference command. The classical objective of the model reference adaptive control problem is to design an adaptive feedback control law such that the state vector $x(t)$ follows the reference state vector $x_r(t)$ in the presence of system uncertainties captured by the unknown matrices “ W ”.

With this objective in mind, let the feedback control law be given as

$$u(t) = -K_1 x(t) + K_2 c(t) - \hat{W}^T(t) x(t), \quad (6)$$

where $K_1 \in \mathbb{R}^{m \times n}$ and $K_2 \in \mathbb{R}^{m \times m}$ are the nominal feedback and feedforward

gain matrices designed such that $A_r \triangleq A - BK_1$ and $B_r \triangleq BK_2$ hold. In addition, $\hat{W}(t) \in \mathbb{R}^{n \times m}$ is the (online) estimate of W satisfying the weight update laws.

$$\dot{\hat{W}}(t) = \gamma \text{Proj}_m[\hat{W}(t), x(t)e^T(t)PB], \quad \hat{W}(0) = \hat{W}_0, \quad (7)$$

where $\gamma \in \mathbb{R}_+$ is the learning rate, $P \in \mathbb{R}_+^{n \times n}$ is the solution of the Lyapunov equation $0 = A_r^T P + P A_r + R$, $R \in \mathbb{R}_+^{n \times n}$, and $e(t) \triangleq x(t) - x_r(t)$ is the system error state vector. The full definition of the projection operator is given in the Appendix, but it should be noted here that a key function of the projection operator is to provide robustness with respect to the parametric uncertainties¹⁰ represented by “ W ”. This is accomplished by enforcing uniform bounds on the adaptive parameters “ $\hat{W}(t)$ ”.

Using Eqs. 4, 5, and 6, the system error dynamics can then be put into the form

$$\dot{e}(t) = A_r e(t) - B \tilde{W}^T(t) x(t), \quad e(0) = e_0, \quad (8)$$

where $\tilde{W}(t) \triangleq \hat{W}(t) - W \in \mathbb{R}^{n \times m}$.

Remark 3.1 *From Eq. 8, the weight update law Eq. 7 can be easily derived using the Lyapunov function candidate $\mathcal{V}(e, \tilde{W}) = e^T P e + \gamma^{-1} \text{tr} \tilde{W}^T \tilde{W}$.¹⁰⁻¹² Specifically, from the time derivative of this Lyapunov function (i.e., $\dot{\mathcal{V}}(e(t), \tilde{W}(t)) \leq -e^T(t) R e(t) \leq 0$), one can conclude the solution $(e(t), \tilde{W}(t))$ is bounded for all time. Furthermore, one can then show $\ddot{\mathcal{V}}(e(t), \tilde{W}(t))$ is bounded such that invoking Barbalat’s lemma¹³ it can be concluded that $\lim_{t \rightarrow \infty} \dot{\mathcal{V}}(e(t), \tilde{W}(t)) = 0$. This consequently shows that $e(t) \rightarrow 0$ as $t \rightarrow \infty$, thereby achieving the classical objective of the model reference adaptive control problem.*

4. Expanded Reference Model for High-Order Actuator Dynamics

A major challenge for the implementation of model reference adaptive control architectures is the exclusion of actuator dynamics in the theoretical development. This is done by making the assumption that the actuator dynamics are fast enough such that the actuation system is properly applying the desired control signal. In this section, we introduce the proposed adaptive control architecture that allows for the

trajectories of the LTV projectile dynamics represented by Eq. 4 to follow the desired reference model trajectories in the presence of high-order actuator dynamics. In particular, we rewrite Eq. 4 as

$$\dot{x}(t) = Ax(t) + B(v(t) + W^T x(t)), \quad x(0) = x_0, \quad (9)$$

where the control signal $u(t)$ as in Eq. 4 is now replaced with $v(t)$ representing the measurable output of the actuator dynamics given by

$$\begin{aligned} \dot{x}_c(t) &= Fx_c(t) + Gu(t), \quad x_c(0) = x_{c0}, \\ v(t) &= Hx_c(t), \end{aligned} \quad (10)$$

with $x_c(t) \in \mathbb{R}^p$ being the actuator state vector, $F \in \mathbb{R}^{p \times p}$ being a Hurwitz actuator state matrix, $G \in \mathbb{R}^{p \times m}$ being the actuator input matrix, and $H \in \mathbb{R}^{m \times p}$ being the actuator output matrix.

To account for the actuator dynamics given by Eq. 10, we design an expanded reference model^{4,7} as

$$\underbrace{\begin{bmatrix} \dot{x}_r(t) \\ \dot{x}_{c_r}(t) \end{bmatrix}}_{\dot{z}_r(t)} = \underbrace{\begin{bmatrix} A + B\hat{W}^T(t) & BH \\ -G(K_1 + \hat{W}^T(t)) & F - GK_3 \end{bmatrix}}_{F_r(\hat{W}(t))} \underbrace{\begin{bmatrix} x_r(t) \\ x_{c_r}(t) \end{bmatrix}}_{z_r(t)} + \underbrace{\begin{bmatrix} 0_{n \times m} \\ GK_2 \end{bmatrix}}_{G_r} c(t), \quad (11)$$

where $K_1 \in \mathbb{R}^{m \times n}$ and $K_2 \in \mathbb{R}^{m \times m}$ are the nominal gains designed such that $A_r = A - BK_1$ is Hurwitz, $B_r = BK_2$ with K_2 being nonsingular, and $-EA_r^{-1}B_r = I$ with $E \in \mathbb{R}^{m \times n}$ being a matrix that allows a user to select a subset $x(t)$ to follow $c(t)$. In addition, $K_3 \in \mathbb{R}^{m \times p}$ is an additional gain matrix and $\hat{W}(t) \in \mathbb{R}^{n \times m}$ is the estimate of W for which the weight update laws are introduced later.

Next, to achieve tracking of the expanded reference model Eq. 11, let the feedback control law be given by

$$u(t) = -K_1 x(t) + K_2 c(t) - K_3 \hat{x}_c(t) - \hat{W}^T(t)x(t), \quad (12)$$

where $\hat{W}(t)$ satisfies the weight update law

$$\dot{\hat{W}}(t) = \gamma \text{Proj}_m[\hat{W}(t), x(t)\tilde{z}^T(t)\mathcal{P}\mathcal{B}], \quad \hat{W}(0) = \hat{W}_0, \quad (13)$$

with $\gamma \in \mathbb{R}_+$ being the learning rate, $\tilde{z}(t) = [e^T(t), (\hat{x}_c^T(t) - x_{cr}^T(t))]^T \in \mathbb{R}^{n+p}$ being the augmented error of the system error state vector $e(t) \in \mathbb{R}^n$ and the actuator state estimate error, $\mathcal{P} \in \mathbb{R}_+^{(n+p) \times (n+p)}$ being a solution of a matrix inequality given by Eq. 16, and $\mathcal{B} = [B^T, 0_{m \times p}]^T \in \mathbb{R}^{(n+p) \times m}$. In addition, the projection bounds are defined such that $\hat{w}_{\min, i+(j-1)n} \leq [\hat{W}(t)]_{ij} \leq \hat{w}_{\max, i+(j-1)n}$, for $i = 1, \dots, n$ and $j = 1, \dots, m$. Furthermore, since the actuator state is not measurable, an observer is used to estimate the actuator state. The observer is designed as

$$\dot{\hat{x}}_c(t) = F\hat{x}_c(t) + Gu(t) + L(v(t) - H\hat{x}_c(t)), \quad \hat{x}_c(0) = \hat{x}_{c0}, \quad (14)$$

where $L \in \mathbb{R}^{p \times m}$ is a gain matrix designed such that $F - LH$ is Hurwitz.

As noted previously, the last part of the proposed adaptive control architecture is obtaining the solution \mathcal{P} . This is done using linear matrix inequalities (LMIs). The main feature of this is that one can determine ahead of time for given projection bounds \hat{W}_{\max} for the elements of $\hat{W}(t)$ and the parameters of the actuator dynamics contained within F , G , and H , that the actuator dynamics are sufficiently fast enough to suppress the effect of the considered system uncertainties. For this purpose, let $\overline{W}_i \in \mathbb{R}^{n \times m}$ represent all the possible variations in $\hat{W}(t)$. Now, let

$$\mathcal{A}_i = \begin{bmatrix} A + B\overline{W}_i^T + \frac{\epsilon}{2}I_n & BH \\ -G(K_1 + \overline{W}_i^T) & F - GK_3 + \frac{\epsilon}{2}I_p \end{bmatrix}, \quad (15)$$

be the corners of the hypercube constructed from all the permutations of \overline{W}_i , where $\epsilon \in \mathbb{R}_+$ is an additional design parameter. For given actuator dynamics represented by F , G , and H , one can then solve the LMI given by

$$\mathcal{A}_i^T \mathcal{P} + \mathcal{P} \mathcal{A}_i < 0, \quad \mathcal{P} > 0, \quad (16)$$

to calculate \mathcal{P} , which is then used in the weight update law (Eq. 13).

5. Simulation Results

In this section, we present the simulation studies conducted on the LTV projectile model presented in Section 3. We consider a flight configuration at Mach 2 and sea level and a second-order actuator model such that

$$F = \begin{bmatrix} 0 & 1 \\ -\omega_n^2 & -2\zeta\omega_n \end{bmatrix}, \quad G = \begin{bmatrix} 0 \\ 1 \end{bmatrix}, \quad H = [\omega_n^2 \quad 0], \quad (17)$$

where ω_n is the natural frequency and ζ is the damping ratio. For this study, we selected an actuator model such that $\zeta = 1$ and $\omega_n = 250$ rad/s. The uncertainties considered emulate a 200% change in the aerodynamic stability coefficient C_{m_α} and a 1000% change in the pitch damping coefficient C_{m_q} . These are made large to make the uncertain projectile model, with a nominal control, unstable. The initial conditions are all set to zero.

Linear quadratic regulator theory¹⁴ is used to design the nominal controller gains. The feedback gain matrix K_1 and the gain K_3 are tuned simultaneously using the weighting matrices $Q = \text{diag}([0.1, 100, 100, 100])$ to penalize the states and $R = 1000$ to penalize the control input. This results in $K_1 = [9.5682, 0.2107]$ and $K_3 = 10^4 \times [6.2299, 0.0112]$, and gives a desirable 79.2° phase margin and a crossover frequency of 173 rad/s. The feedforward gain K_2 is designed such that the desired pitch acceleration $\dot{w}(t)$ is followed. For this purpose, using $E = [0, 1]$, the gain K_2 is calculated as $K_2 = -(EA_r^{-1}B)^{-1} = 0.3198$. Furthermore, the observer gain L , is also designed using linear quadratic regulator theory with the weighting matrices $Q_L = \text{diag}([1000, 1000])$ and $R_L = 0.01$ resulting in $L = [316.23, -0.684]^T$. Figures 3 and 4 show the nominal baseline control performance for the case in which there is no system uncertainty and then with the uncertainty in the aerodynamic stability coefficient C_{m_α} and the pitch damping coefficient C_{m_q} included. It can be seen that when the uncertainty is added, the nominal control is not sufficient to provide stability for the projectile flight control.

In the proposed controller, we use the feasible solution \mathcal{P} from the LMI analysis highlighted in the previous section. This is obtained for the considered example with $\epsilon = 0.35$ and the selected elemental projection bounds given by $0 \leq [\hat{W}(t)]_1 \leq 1.7952$ and $-0.0994 \leq [\hat{W}(t)]_2 \leq 0$. The projection bounds are selected to provide a 5% tolerance for the estimation of the unknown parameters in the uncertainty

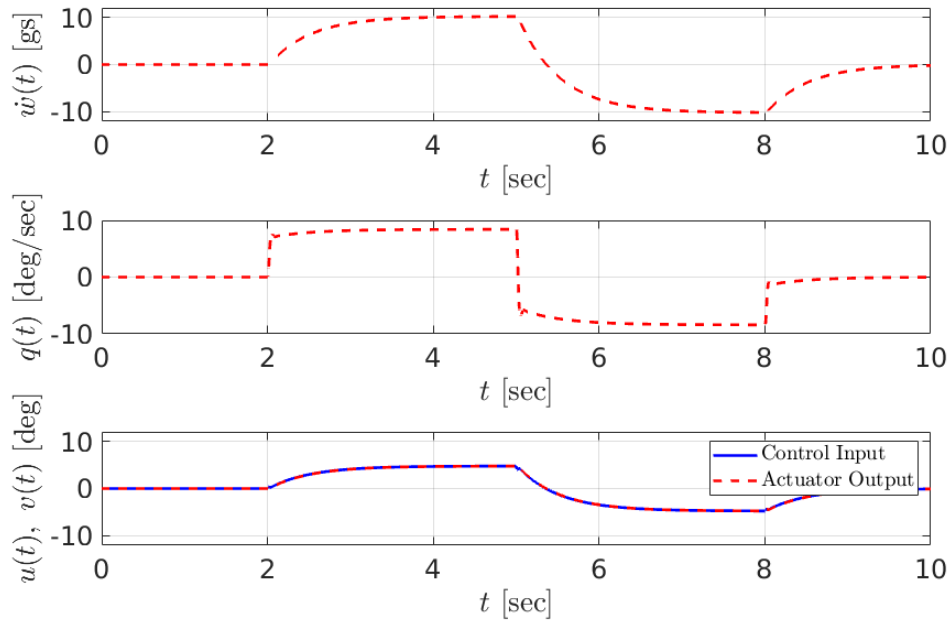


Fig. 3 Nominal baseline control performance with no system uncertainty

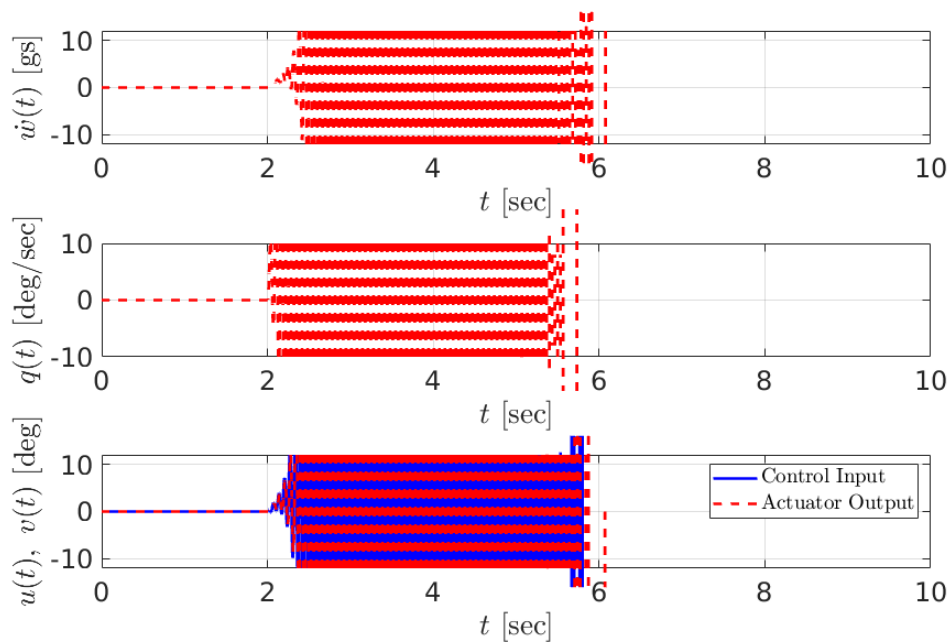


Fig. 4 Nominal baseline control performance with system uncertainty included. Projectile response is unstable as expected.

matrix “ W ”. The learning gain for the adaptive control is set as $\gamma = 5000$.

Figure 5 shows the control performance. It can be seen that in the presence of system uncertainties, the adaptive control allows for quick tracking of the reference model trajectories in the pitch acceleration $\dot{w}(t)$ and the pitch rate $q(t)$, and the actuator is fast enough that the output $v(t)$ is very close to the desired control input $u(t)$. This is to be expected since the LMI analysis produces a feasible solution \mathcal{P} for the considered actuator dynamics and system uncertainties. Figures 6–8 show the results of further increasing the uncertainty in the pitch damping coefficient C_{m_q} to 1500%, 2000%, and 2500%, respectively, of the true value. For the first two increases, the LMI analysis provides a feasible solution \mathcal{P} , implying that the actuator dynamics are still fast enough to provide the appropriate control to suppress the increased level of uncertainty. This can be seen in Figs. 6 and 7. While there is increased oscillation, the overall result remains stable and the projectile trajectories track the reference system. However, when the uncertainty is increased by 2500%, the LMI analysis does not produce a feasible solution \mathcal{P} . This implies the actuator is not fast enough for this level of uncertainty as can be seen in Fig. 8. It can be noted from Fig. 8 that while the projectile system eventually stabilizes and tracks the desired reference trajectories, the performance is severely degraded and would be undesirable. This alludes to some conservatism in the proposed LMI approach. Through further increase in the uncertainty, it was found that the instability occurred after a 2650% increase in the pitch damping coefficient C_{m_q} .

6. Conclusion

In this work, a new model reference adaptive control architecture was documented for uncertain dynamical systems with high-order actuator dynamics. The proposed approach uses an expanded reference model constructed with the actuator model included. This allows for the proper application of the adaptive control signal. An LMI analysis is then used to compute a priori that the actuator dynamics are in fact fast enough to suppress the considered level of uncertainty. This results in a feasible solution \mathcal{P} that is used in the weight estimate law. Simulation studies were carried out on the DEVCOM ARL LTV projectile model to elucidate the proposed control architecture. Future research can include extending the scope of the proposed approach to the case in which the system uncertainties are nonlinear such that a wider class of practical applications can be considered.

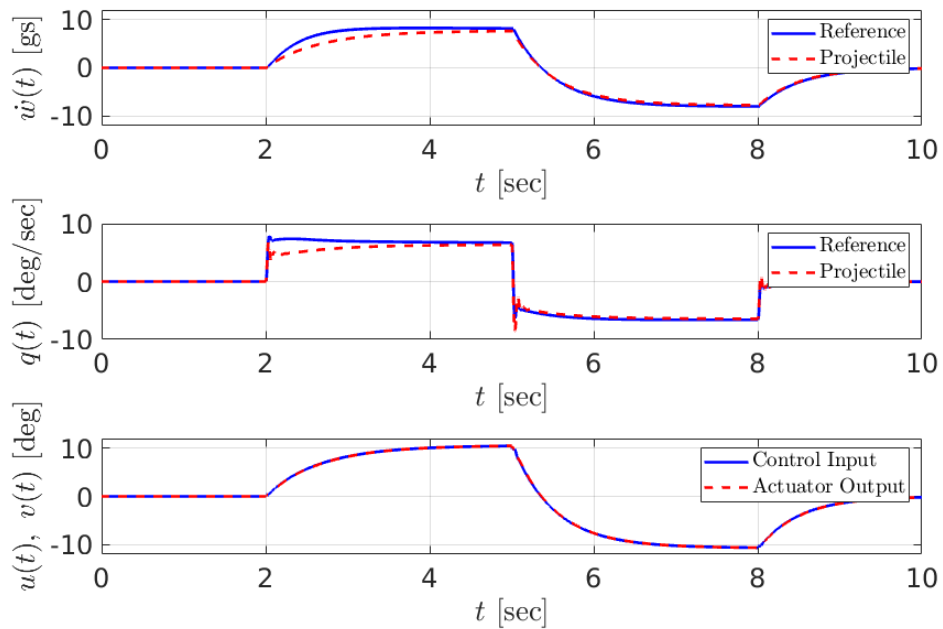


Fig. 5 Expanded reference model control performance for 1000% increase in the uncertainty of the pitch damping coefficient C_{m_q}

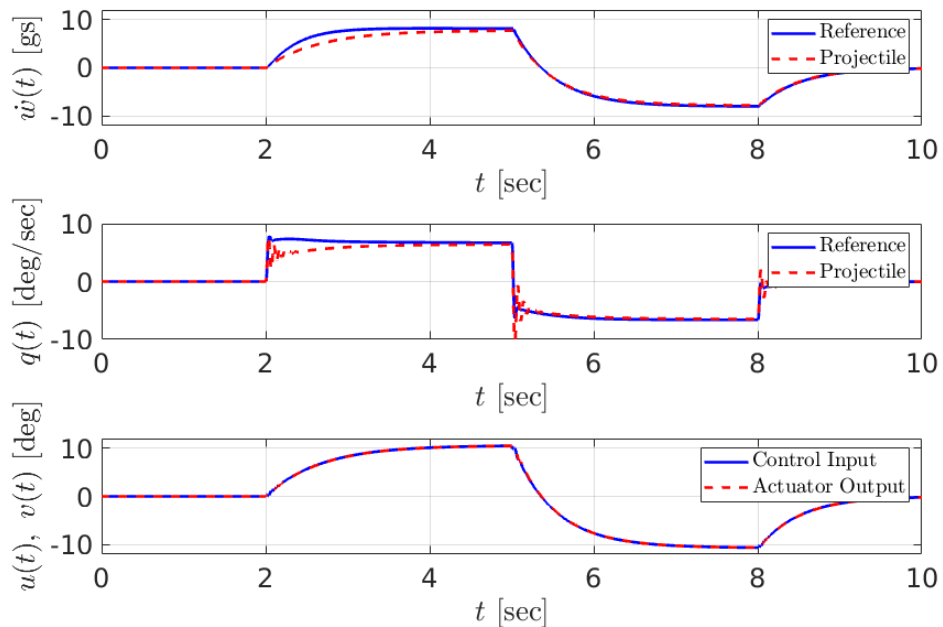


Fig. 6 Expanded reference model control performance for 1500% increase in the uncertainty of the pitch damping coefficient C_{m_q}

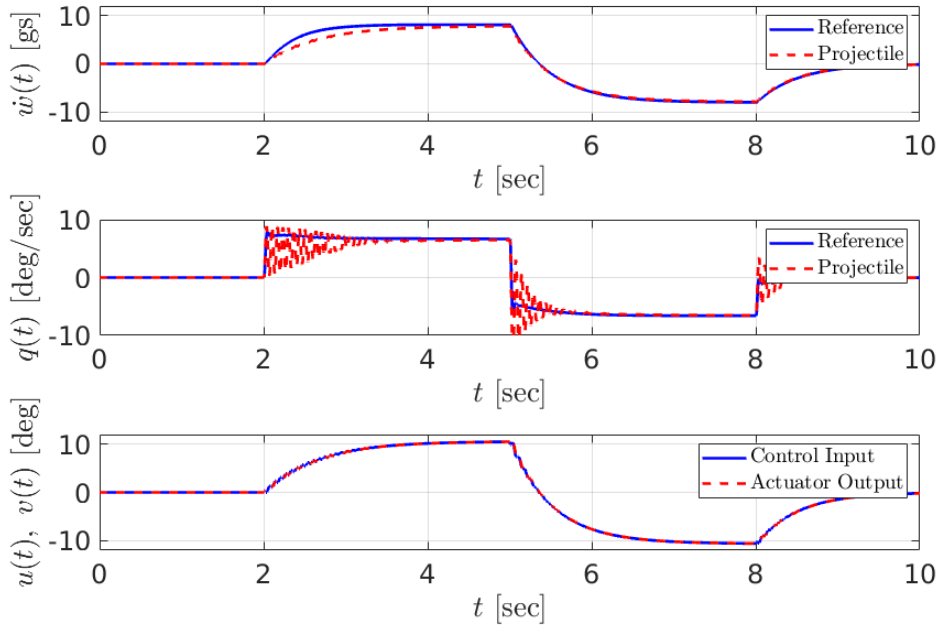


Fig. 7 Expanded reference model control performance for 2000% increase in the uncertainty of the pitch damping coefficient C_{m_q}

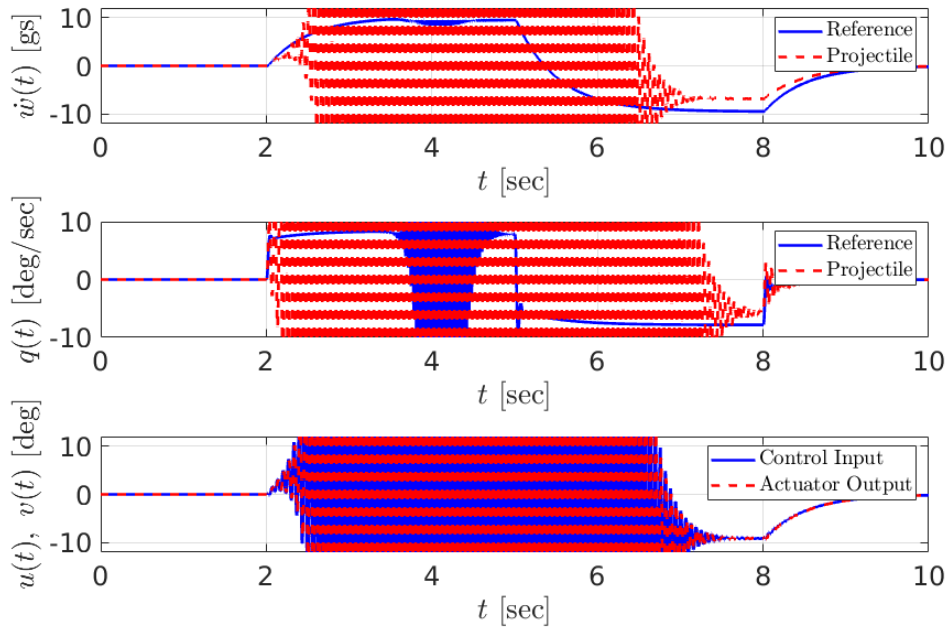


Fig. 8 Expanded reference model control performance for 2500% increase in the uncertainty of the pitch damping coefficient C_{m_q}

7. References

1. Vasile JD, Bryson J, Fresconi F. Aerodynamic design optimization of long range projectiles using missile datcom. AIAA Scitech 2020 Forum; 2020 Jan. Paper No.: AIAA 2020-1762.
2. Vasile JD, Bryson J, Gruenwald BC, Fairfax L, Strohm L, Fresconi F. A multi-disciplinary approach to design long range guided projectiles. AIAA Scitech 2020 Forum; 2020 Jan. Paper No.: AIAA 2020-1993.
3. Bryson J, Vasile JD, Gruenwald BC, Fresconi F. Control surface design analysis and actuation requirements development for munitions. AIAA Scitech 2020 Forum; 2020 Jan. Paper No.: AIAA 2020-0020.
4. Gruenwald BC, Bryson J. Adaptive control for a guided projectile using an expanded reference model. AIAA Scitech 2020 Forum; 2020 Jan. Paper No.: AIAA 2020-1822.
5. Fairfax LD, Vasile JD, Strohm L, Fresconi F. Trajectory shaping for quasi-equilibrium glide in guided munitions. AIAA Scitech 2020 Forum; 2020 Jan. Paper No.: AIAA 2020-0021.
6. Gruenwald BC, Yucelen T, Dogan KM, Muse JA. A new adaptive control architecture for uncertain dynamical systems with actuator dynamics: Beyond pseudo-control hedging. AIAA Guidance, Navigation, and Control Conference. 2018;.
7. Gruenwald BC, Yucelen T, Dogan KM, Muse JA. Expanded reference models for adaptive control of uncertain systems with actuator dynamics. *Journal of Guidance, Control, and Dynamics*. 2020;43(3):475–489.
8. Vasile J, Sahu J. Roll orientation–dependent aerodynamics of a long-range projectile. DEVCOM Army Research Laboratory; 2020 Aug. Report No.: ARL-TR-9017.
9. Vasile JD, Bryson JT, Sahu J, Paul JL, Gruenwald BC. Aerodynamic dataset generation of a long-range projectile. DEVCOM Army Research Laboratory; 2020 Aug. Report No.: ARL-TR-9019.
10. Lavretsky E, Wise KA. Robust adaptive control. Springer-Verlag; 2013.

11. Ioannou PA, Sun J. Robust adaptive control. Courier Corporation; 2012.
12. Narendra KS, Annaswamy AM. Stable adaptive systems. Courier Corporation; 2012.
13. Khalil HK. Nonlinear systems. Prentice Hall; 2002.
14. Lewis FL, Syrmos VL. Optimal control. Wiley; 1995.

Appendix. Projection Operator

Definition A.1 Consider a convex hypercube in the form $\Omega = \{\theta \in \mathbb{R}^n : (\theta_i^{\min} \leq \theta_i \leq \theta_i^{\max})_{i=1,2,\dots,n}\}$, where $\Omega \in \mathbb{R}^n$, and θ_i^{\min} and θ_i^{\max} , respectively, represent the minimum and maximum bounds for the i^{th} component of the n -dimensional parameter vector θ . Furthermore, for a sufficiently small positive constant ϵ_0 , consider another hypercube in the form $\Omega_\epsilon = \{\theta \in \mathbb{R}^n : (\theta_i^{\min} + \epsilon_0 \leq \theta_i \leq \theta_i^{\max} - \epsilon_0)_{i=1,2,\dots,n}\}$, where $\Omega_\epsilon \subset \Omega$. The projection operator $\text{Proj} : \mathbb{R}^n \times \mathbb{R}^n \rightarrow \mathbb{R}^n$ is then defined component-wise by

$$\text{Proj}(\theta, y) \triangleq \begin{cases} \left(\frac{\theta_i^{\max} - \theta_i}{\epsilon_0} \right) y_i, & \text{if } \theta_i > \theta_i^{\max} - \epsilon_0 \text{ and } y_i > 0, \\ \left(\frac{\theta_i - \theta_i^{\min}}{\epsilon_0} \right) y_i, & \text{if } \theta_i < \theta_i^{\min} + \epsilon_0 \text{ and } y_i < 0, \\ y_i, & \text{otherwise,} \end{cases}$$

where $y \in \mathbb{R}^n$.

Based on Definition A.1 and $\theta^* \in \Omega_\epsilon$, one can show the inequality

$$(\theta - \theta^*)^T (\text{Proj}(\theta, y) - y) \leq 0,$$

holds for $\theta \in \Omega$ and $y \in \mathbb{R}^n$ [10]. In addition, we use a generalization of this definition to matrices for (Eq. 13 in main text) as $\text{Proj}_m(\Theta, Y) = (\text{Proj}(\text{col}_1(\Theta), \text{col}_1(Y)), \dots, \text{Proj}(\text{col}_m(\Theta), \text{col}_m(Y)))$, where $\Theta \in \mathbb{R}^{n \times m}$, $Y \in \mathbb{R}^{n \times m}$, and $\text{col}_i(\cdot)$ denotes the i -th column operator. In this case, for a given matrix Θ^* , it follows that

$$\begin{aligned} \text{tr} \left[(\Theta - \Theta^*)^T (\text{Proj}_m(\Theta, Y) - Y) \right] &= \sum_{i=1}^m \left[\text{col}_i(\Theta - \Theta^*)^T (\text{Proj}(\text{col}_i(\Theta), \text{col}_i(Y)) \right. \\ &\quad \left. - \text{col}_i(Y)) \right] \leq 0, \end{aligned}$$

holds.

List of Symbols, Abbreviations, and Acronyms

ARL	Army Research Laboratory
CG	center of gravity
DEVCOM	US Army Combat Capabilities Development Command
L/D	length-to-diameter ratio
LMI	linear matrix inequality
LTV	Laboratory Technology Vehicle

MATHEMATICAL SYMBOLS:

\mathbb{R}	the set of real numbers.
\mathbb{R}^n	the set of $n \times 1$ real column vectors.
$\mathbb{R}^{n \times m}$	the set of $n \times m$ real matrices.
\mathbb{R}_+	the set of positive real numbers.
$\mathbb{R}_+^{n \times n}$	the set of $n \times n$ positive-definite real matrices.
$0_{n \times m}$	the $n \times m$ matrix of all zeros.
I_n	the $n \times n$ identity matrix.
\triangleq	the equality by definition.

MATHEMATICAL OPERATORS:

$(\dot{\cdot})$	the overdot denotes the time-derivative.
$(\cdot)^T$	the transpose operator.
$(\cdot)^{-1}$	the inverse operator.
$\text{tr}(\cdot)$	the trace operator.

1 DEFENSE TECHNICAL
(PDF) INFORMATION CTR
DTIC OCA

1 DEVCOM ARL
(PDF) FCDD RLD DCI
TECH LIB

18 DEVCOM ARL
(PDF) FCDD RLW A
F E FRESCONI
FCDD RLW W
T SHEPPARD
FCDD RLW WD
J T BRYSON
B C GRUENWALD
L STROHM
B BURCHETT
I CELMINS
J DESPIRITO
L FAIRFAX
J PAUL
J D VASILE
FCDD RLW WA
N TRIVEDI
FCDD RLW WB
J SADLER
FCDD RLW WC
M MINNICINO
FCDD RLW WE
M ILG
B TOPPER
D EVERSON
FCDD RLW WF
E RIGAS